Research article

Eye-hand-workspace calibration using laser pointer projection on plane surface

Jwu-Sheng Hu and Yung-Jung Chang
Department of Electrical and Control Engineering, National Chiao Tung University, Hsinchu, Taiwan and
Mechanical and Systems Research Laboratories, Industrial Technology Research Institute, Hsinchu, Taiwan

Abstract
Purpose – The purpose of this paper is to propose a calibration method that can calibrate the relationships among the robot manipulator, the camera and the workspace.
Design/methodology/approach – The method uses a laser pointer rigidly mounted on the manipulator and projects the laser beam on the work plane. Nonlinear constraints governing the relationships of the geometrical parameters and measurement data are derived. The uniqueness of the solution is guaranteed when the camera is calibrated in advance. As a result, a decoupled multi-stage closed-form solution can be derived based on parallel line constraints, line/plane intersection and projective geometry. The closed-form solution can be further refined by nonlinear optimization which considers all parameters simultaneously in the nonlinear model.
Findings – Computer simulations and experimental tests using actual data confirm the effectiveness of the proposed calibration method and illustrate its ability to work even when the eye cannot see the hand.
Originality/value – Only a laser pointer is required for this calibration method and this method can work without any manual measurement. In addition, this method can also be applied when the robot is not within the camera field of view.

Keywords Robotics, Lasers, Calibration, Hand/eye calibration, Manipulator, Camera, Laser pointer, Closed-form solution, Optimization

Paper type Research paper

Introduction

Robot hand-eye coordination systems have many industrial applications because they provide the reliability and flexibility for tasks such as automatic assembly, welding, and pick and place. Calibrations often performed to maximize performance in such systems, including robot calibration, camera calibration, hand/eye calibration, and robot/workspace calibration. This work proposes a method of simultaneously calibrating eye/hand/workspace by using a laser pointer projection on the working plane.

Classic hand/eye calibration methods use a known-dimension 3D reference object or a precisely printed 2D pattern. The camera poses can be determined by inversely projecting the features of the reference in an image in the camera calibration stage. The basic approaches are to solve the hand-eye transformation equation in the form, $AX = XB$, which was first introduced by Shiu and Ahmad (1987, 1989). Tsai and Lenz (1988, 1989) developed the closed-form solution by decoupling the problem into two stages, rotation and then translation. Quaternion-based approaches, such as those introduced by Chou and Kamel (1988), Zhuang and Roth (1991) and Horaud and Dornaika (1995), lead to a linear form to solve rotation relationships. To avoid error propagation from the rotation stage to the translation stage, Zhuang and Shiu (1993) developed a nonlinear optimization method with respect to three Euler angles of a rotation and a translation vector. For simultaneous consideration of hand/eye and robot/world problems, Zhuang *et al.* (1994) introduced the transformation chain in the general form, $AX = YB$, and presented a linear solution based on quaternions and the linear least square technique. A similar work by Dornaika and Horaud (1998) included a closed-form solution and a nonlinear minimization solution. Motta *et al.* (2001) introduced a modification of Tsai's camera calibration method (1987) to obtain several camera poses by the eye-in-hand configuration and introduced a robot calibration method using the camera poses. Motai and Kosaka (2008) present a procedure of hand-eye calibration by slightly modifying Tsai's camera calibration (1987) and adopting Shiu and Ahmad's hand-eye calibration method (1989). Wang (1992) was the first to present the hand/eye calibration that can be achieved just using a single point at an unknown position. The other works using a single point, such as Xu *et al.* (2008) and Jordt *et al.* (2009), include finding camera intrinsic parameters. Gatla *et al.* (2007) considered the calibration of the special case of pan-tilt cameras attached to the hand using a single point. In their experiment, a laser distance sensor is attached on another robot manipulator to form a static point as a reference on the surface, but they actually do not use the property of the laser beam in their method. Andreff *et al.* (2001) was based on the well-known

The current issue and full text archive of this journal is available at
www.emeraldinsight.com/0143-991X.htm

Industrial Robot: An International Journal
39/2 (2012) 197–207
 [ISSN 0143-991X]
[DOI 10.1108/01439911211201663]

Industrial Robot: An International Journal
Volume 39 · Number 2 · 2012 · 197–207

structure-from-motion method. It provided a linear formulation and several solutions for combining specific end-effector motions. This kind of methods is useful for online calibration but have a risk of feature mismatching that may cause disastrous error.

Most existing hand-eye calibration methods are dealing with the hand-in-eye configuration. Actually, many of them are applicable in either eye-in-hand (or eye-on-hand) or eye-to-hand configurations. Dornaika and Horaud (1998) presented the formulation to deal with the calibration problem for the both configurations and showed that these two configurations are actually identical. However, in the eye-to-hand configuration, this identity is tenable only when the hand can be viewed by the eye. This limits installation flexibility and potential applications. For example, to sort products on a moving conveyor, the camera is often placed at a distance from the arm to compensate for image processing delay and to avoid interference when tracking targets on a rapidly moving conveyor belt. In a catching ball system (Hu *et al.*, 2010), cameras focus on the region of the initial trajectory of the ball and may not see the arm. Sun *et al.* (2004) introduced a robot-world calibration method using a triple laser device. Although their method enables eye-to-hand calibration in this situation, it requires a specially designed triple-laser device, which limits flexibility of system arrangement, and the spatial relationship from working plane to camera must be known in advance.

The calibration reference used in this method substantially differs from the existing methods mentioned above. A major advantage of this approach is that the laser pointer enables calibration even when the eye cannot see the hand. Restated, this technique increases the working range of hand-eye coordination. A general eye-to-hand calibration method using a laser pointer mounted on the end-effector was proposed in Hu and Chang (2011). To deal with uncalibrated cameras, the method has to rely on projecting the laser spot on several non-parallel planes to arrive at a unique solution. This study considers the case in which intrinsic parameters of the camera are already known. As a result, only one plane is needed and if the working plane is assigned, this method enables simultaneous eye-hand-workspace calibration. Ghosh *et al.*'s (1998) method considers calibrating the workspace together, but their method needs another sensor and has to assume that the working plane and the horizontal plane of the robot base are parallel. Our proposed method takes the advantage of robot's mobility and dexterity. By manipulating the robot to project the laser beam on the plane, a batch of related image positions of light spots is extracted from camera images. Since the laser is mounted rigidly and the plane is fixed, the geometrical parameters and measurement data must obey certain nonlinear constraints, and the parameter solutions can be estimated accordingly. A closed-form solution is developed by decoupling nonlinear equations into linear forms to compute all initial values. Therefore, the proposed calibration method does not require manual estimation of unknown parameters. To achieve high accuracy, a nonlinear optimization method that considers all parameters at a time is then implemented to refine the estimation. This approach does not need manual installation of a pattern or an object in the workspace; hence, it will enable fully automatic calibration.

The remainder of this paper is organized as follows. First, an overview of the approach is given. The basic idea of using system redundant information to achieve calibration is presented. Following that are details of the closed-form solution and nonlinear optimization based on the geometrical constraints. A recommended procedure of implement of this approach is provided. The proposed method is then discussed with experimental results obtained by simulations and using real data. The results are compared with the results of using Dornaika and Horaud's method (1998) in the simulations. Finally, a conclusion is given.

Overview of the approach

The objective of calibration is to reduce systematic errors by correcting the parameters. The geometrical relationships using a laser pointer to calibrate an eye-to-hand system is illustrated here. Figure 1 shows the overall configuration of an eye-to-hand system, in which a laser pointer is attached to the end-effector for calibration and a working plane is in front of the camera.

The camera model used is the pin-hole type with considering lens distortion. A 2D position in an image is denoted as $\mathbf{m} = [u, v]^T$, and its homogeneous coordinate is defined as $\tilde{\mathbf{m}} = [u, v, 1]^T$. A 3D position in the camera frame is denoted as $\mathbf{x}_C = [x_C, y_C, z_C]^T$:

$$\tilde{\mathbf{m}} = \mathbf{K} \cdot \begin{bmatrix} x_d \\ y_d \\ 1 \end{bmatrix} \quad \text{with } \mathbf{K} = \begin{bmatrix} f_u & \alpha_c \cdot f_u & u_0 \\ 0 & f_v & v_0 \\ 0 & 0 & 1 \end{bmatrix} \tag{1}$$

where $\mathbf{K}$, the intrinsic matrix, including two focal lengths (f_u, f_v), two principal points (u_0, v_0), and a skew coefficient α_c, and:

$$\begin{bmatrix} x_d \\ y_d \end{bmatrix} = (1 + \kappa_1 \|\mathbf{x}_r\|^2 + \kappa_2 \|\mathbf{x}_r\|^4)\mathbf{x}_r + \begin{bmatrix} 2\rho_1 x_r y_r + \rho_2(\|\mathbf{x}_r\|^2 + 2x_r^2) \\ \rho_1(\|\mathbf{x}_r\|^2 + 2y_r^2) + 2\rho_2 x_r y_r \end{bmatrix} \tag{2}$$

where $\mathbf{x}_r = [x_C/z_C \quad y_C/z_C]^T$ is the ray direction from the camera, κ_1 and κ_2 are radial distortion parameters, and ρ_1 and ρ_2 are tangential distortion parameters (Brown, 1971). Since the camera calibration is fundamental in machine vision, there are rich literatures and resources on camera calibration.

Figure 1 Overview of an eye-to-hand system with a laser pointer

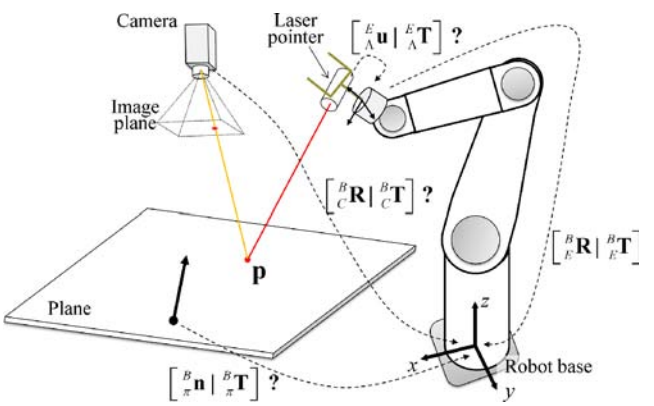

The direct linear transformation (DLT) (Abdel-Aziz and Karara, 1971; Shapiro, 1978) is applied to camera calibration to obtain linear solution. Bacakoglu and Kamel (1997) adopted the DLT method and the nonlinear estimation, and developed methods to refine homogeneous transformation between the two steps. Methods based on DLT method basically need a 3D reference. Tsai (1987) developed a radial alignment constraint (RAC) based method using a 2D pattern. Zhuang *et al.* (1993) improved the Tsia's RAC method and utilized robot mobility to deal with multiple planes. Zhang (2000) provided a flexible method which can handle data of different poses of a planar pattern and does not need any robot or linear table. An excellent toolbox named *Camera Calibration Toolbox for Matlab* (Bouguet, 2010) based on Zhang's method (2000) is available online and is used in this work.

The rigid transformation from one coordinate system to another coordinate is determined by a rotation matrix $\mathbf{R}$ and a translation vector $\mathbf{T}$. A point ${}^{a}\mathbf{p}$ in the a frame is transformed into the b frame via:

$$ {}^{b}\mathbf{p} = {}^{b}_{a}\mathbf{R} \cdot {}^{a}\mathbf{p} + {}^{b}_{a}\mathbf{T} \tag{3} $$

where $\mathbf{R}$ is a 3×3 rotation matrix and $\mathbf{T}$ is a 3×1 translation vector. The rotation matrix can be derived by the direction cosine matrix, $\mathbf{R}(\theta,\phi,\varphi)$, and its rotation sequence is Z-Y-X, where θ is z-axis rotation, ϕ is y-axis rotation, and φ is x-axis rotation. In general, the robot base coordinate system is identical to the world coordinate system for the overall system in the following context. Transformation from the end-effector frame to the robot base frame is by a rotation matrix ${}^{B}_{E}\mathbf{R}$ and a translation vector ${}^{B}_{E}\mathbf{T}$, and they can be derived from robot forward kinematics. The relationships between the robot base and the camera are denoted as $\left[{}^{B}_{C}\mathbf{R} | {}^{B}_{C}\mathbf{T}\right]$, and these relationships are parts of the calibration target.

Another calibration target is the pose of the workspace, which is a plane. The plane is defined by a normal vector ${}^{B}_{\pi}\mathbf{n}$ and a point ${}^{B}_{\pi}\mathbf{T}$ on the plane in the robot base coordinate system. This plane in 3D space has three degrees of freedom and can be generally defined as:

$$ {}^{B}_{\pi}\mathbf{a} = \left({}^{B}_{\pi}\mathbf{n}^{T} \cdot {}^{B}_{\pi}\mathbf{T}\right){}^{B}_{\pi}\mathbf{n}. \tag{4} $$

Figure 2 shows the relationships between the laser pointer and the end-effector. In the coordinate system of the end-effector,

Figure 2 The laser beam with respect to the end-effector

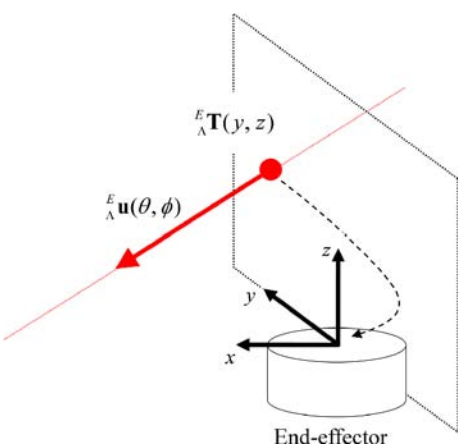

the direction of the laser beam is described as a unit vector ${}^{E}_{\Lambda}\mathbf{u}$, which has two degrees of freedom and can be denoted by Euler angles as:

$$ {}^{E}_{\Lambda}\mathbf{u} = \left[\cos{}^{E}_{\Lambda}\theta \sin{}^{E}_{\Lambda}\phi \quad \sin{}^{E}_{\Lambda}\theta \sin{}^{E}_{\Lambda}\phi \quad \cos{}^{E}_{\Lambda}\phi\right]^{T} \tag{5} $$

where ${}^{E}_{\Lambda}\theta \in [0, 2\pi)$ is the z-axis rotation angle and ${}^{E}_{\Lambda}\phi \in [0, \pi]$ is the angle between z-axis and ${}^{E}_{\Lambda}\mathbf{u}$. Without loss of generality, let the laser origin ${}^{E}_{\Lambda}\mathbf{T}$ be the point at which the laser beam intersects the x-y plane of the end-effector coordinate system, i.e.:

$$ {}^{E}_{\Lambda}\mathbf{T} = {}^{E}_{\Lambda}[0 \quad y \quad z]^{T}. \tag{6} $$

Otherwise, let ${}^{E}_{\Lambda}\mathbf{T} = {}^{E}_{\Lambda}[x \quad 0 \quad z]^{T}$ or ${}^{E}_{\Lambda}\mathbf{T} = {}^{E}_{\Lambda}[x \quad y \quad 0]^{T}$. These additional laser parameters must then be calibrated. Since the laser pointer is rigidly installed, these parameters do not change under normal operation.

In summary, the calibration targets are hand/eye/workspace relationships and additional laser installation parameters, and camera intrinsic parameters are known a prior. The unknown relationships are labeled with question marks in Figure 1.

In this system, three methods can be used to calculate a laser spot 3D position which the laser beam is projected onto the plane and that laser spot is captured by the camera:

1 *Intersection of the laser beam and plane.* The 3D location of a laser point on a plane is derived via the principle of line/plane intersection. The geometrical constraint is:

$$ \left(d_{L}{}^{B}_{\Lambda}\mathbf{u} + {}^{B}_{\Lambda}\mathbf{T} - {}^{B}_{\pi}\mathbf{a}\right)^{T} \cdot {}^{B}_{\pi}\mathbf{a} = 0 \tag{7} $$

where d_L is the distance from the laser origin to the projected point and:

$$ d_{L} = \frac{\left\|{}^{B}_{\pi}\mathbf{a}\right\| - {}^{B}_{\Lambda}\mathbf{T}^{T} \cdot {}^{B}_{\pi}\mathbf{a}}{{}^{B}_{\Lambda}\mathbf{u}^{T} \cdot {}^{B}_{\pi}\mathbf{a}}. \tag{8} $$

Hence, the 3D position of the laser spot is described as:

$$ {}^{B}\mathbf{p}_{spot} = d_{L}{}^{B}_{\Lambda}\mathbf{u} + {}^{B}_{\Lambda}\mathbf{T}. \tag{9} $$

2 *Intersection of the plane and ray from the camera.* A laser spot is projected onto an image taken by the camera. The ray direction, denoted as $\mathbf{x}_n$, from the origin of the camera frame to the laser spot can be obtained using the pixel position by applying the inverse intrinsic matrix and the undistortion method. According to the principle of line/plane intersection, the geometrical constraint is:

$$ \left({}^{B}_{C}\mathbf{R} \cdot d_{C}{}^{C}_{C}\tilde{\mathbf{x}}_{n} + {}^{B}_{C}\mathbf{T} - {}^{B}_{\pi}\mathbf{a}\right)^{T} \cdot {}^{B}_{\pi}\mathbf{a} = 0 \tag{10} $$

where ${}^{C}\tilde{\mathbf{x}}_{n} = [\mathbf{x}_{n}^{T} \quad 1]^{T}$. Then:

$$ d_{C} = \frac{\left\|{}^{B}_{\pi}\mathbf{a}\right\| - {}^{B}_{C}\mathbf{T}^{T} \cdot {}^{B}_{\pi}\mathbf{a}}{\left({}^{B}_{C}\mathbf{R}{}^{C}\tilde{\mathbf{x}}_{n}\right)^{T} \cdot {}^{B}_{\pi}\mathbf{a}}. \tag{11} $$

Hence, the 3D position of the laser spot is:

$$ {}^{B}\mathbf{p}_{spot} = d_{C} \cdot {}^{B}_{C}\mathbf{R}{}^{C}\tilde{\mathbf{x}}_{n} + {}^{B}_{C}\mathbf{T}. \tag{12} $$

3 *Triangulation of the laser beam and ray from the camera.* Position ${}^{B}\mathbf{p}_{spot}$ can also be determined by triangulation of the laser beam and the camera ray. This position, which is the intersection of two lines, is:

$$ {}^{B}\mathbf{p}_{spot} = d_L {}^{B}_{\Lambda}\mathbf{u} + {}^{B}_{\Lambda}\mathbf{T} = d_C {}^{B}_{C}\tilde{\mathbf{x}}_n + {}^{B}_{C}\mathbf{T}. \quad (13) $$

This leads to the equation:

$$ \begin{bmatrix} {}^{B}\mathbf{u}_L & -{}^{B}\tilde{\mathbf{x}}_n \end{bmatrix} \begin{bmatrix} d_L \\ d_C \end{bmatrix} = {}^{B}_{C}\mathbf{T} - {}^{B}_{\Lambda}\mathbf{T} \quad (14) $$

which can be solved by least squares method.

This analysis indicates the existence of redundant information in this system configuration. The positional differences of the same point derived via the different methods are caused by systematic errors and/or noisy measurements. This implies that the systematic parameters can be estimated by tuning these parameters to reduce the differences of positions, either 3D positions or 2D image positions.

The proposed methods

A closed-form solution is proposed followed by an optimization solution. The optimization problem, which is described later, is nonlinear. To avoid local minimum and to accelerate convergence, accurate initial values are needed. The closed-form solution is derived by exploring the arrangements in the setup. Since no prior guess of parameters is needed, the proposed method can run automatically.

Closed-form solution

Some parts of the closed-form solution are achieved by translating, but not rotating, the end-effector. This pure translational motion can decompose the problem into linear forms according to the constraints of parallel laser beams.

Several orientations of the end-effector with the laser pointer are performed. Under the mth orientation, the end-effector is translated, but not rotated, along several vectors, $\mathbf{j}_{m,n}$'s, and the laser spot on the plane moves along corresponding vectors, $\mathbf{i}_{m,n}$'s, as shown in Figure 3. In the end, the orientations of laser beams corresponding with different hand poses determine the geometric dimensions of the overall system.

The step-by-step of this closed-form solution is clearly described in detail as follows.

Figure 3 Projection of parallel laser beams on a plane

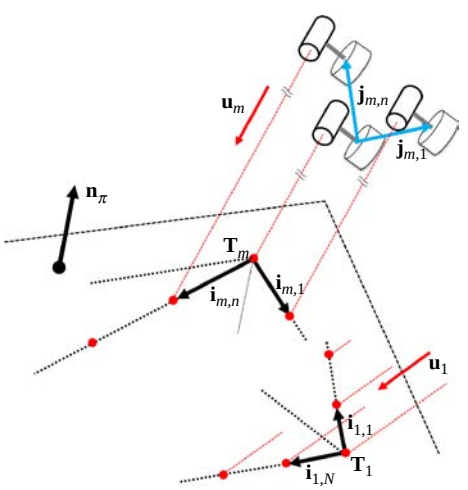

(1) Calculate the ray directions of all points

Each projected laser spot is located in an image, and its direction from the camera is obtained by calculating its inverse projection. With the camera intrinsic parameters, for any point in an image, the ray direction $\mathbf{x}_r$ can then be derived accordingly.

(2) Find homogeneous matrixes, each having an unknown scale factor

Suppose the end-effector moves along a direction (without rotation) that is a linear combination of N translating vectors ($\mathbf{j}_{m,n}$ vectors). The laser spot will move along a vector that is the same linear combination of corresponding vectors ($\mathbf{i}_{m,n}$ vectors). Specifically, under mth rotation and kth translation, the laser spot is at position:

$$ \mathbf{x}_{m,k} = \begin{bmatrix} z \cdot \mathbf{x}_r \\ z \end{bmatrix}_{m,k} = \mathbf{H}_m \begin{bmatrix} \mathbf{w}_{m,k} \\ 1 \end{bmatrix} $$

$$ = \begin{bmatrix} \mathbf{i}_{m,1} & \cdots & \mathbf{i}_{m,N} & \mathbf{T}_m \end{bmatrix} \begin{bmatrix} w_1 \\ \vdots \\ w_N \\ 1 \end{bmatrix}_{m,k} \quad (15) $$

where w_n, $n = 1 \sim N$ are scales of a combination according to end-effector movement, and $\mathbf{H}_m$ is a homogeneous matrix. Let $\bar{\mathbf{h}}_i$ be the ith row of $\mathbf{H}$. A solution for the homogeneous matrix can then be obtained by DLT method (Hartley and Zisserman, 2003). That is:

$$ \mathbf{Q}_\mathbf{H} \cdot \mathbf{x}_\mathbf{H} = \begin{bmatrix} \mathbf{w}_k^T & 0 & -x_r \mathbf{w}_K^T \\ 0 & \mathbf{w}_k^T & -y_r \mathbf{w}_K^T \end{bmatrix} \begin{bmatrix} \bar{\mathbf{h}}_1^T \\ \bar{\mathbf{h}}_2^T \\ \bar{\mathbf{h}}_3^T \end{bmatrix} = 0. \quad (16) $$

For K points, dimension of $\mathbf{Q}_\mathbf{H}$ is $(2K) \times (3N + 3)$, and a unique solution $\mathbf{x}_\mathbf{H}$ exists if $\mathbf{Q}_\mathbf{H}$ is ranked $3N + 2$. The solution is the eigenvector corresponding to the smallest eigenvalue of the matrix $\mathbf{Q}_\mathbf{H}^T \mathbf{Q}_\mathbf{H}$. According to equation (16), the solution has an unknown scalar factor λ, and:

$$ \mathbf{H}_m = \lambda_m \hat{\mathbf{H}}_m = \lambda_m \begin{bmatrix} \hat{\mathbf{i}}_{m,1} & \cdots & \hat{\mathbf{i}}_{m,N} & \hat{\mathbf{T}}_m \end{bmatrix} \quad (17) $$

Scalar factors of M orientations (λ_m, $m = 1 \sim M$) are obtained in the following steps.

(3) Find the normal vector of the plane w.r.t the camera

Since all $\mathbf{i}_{m,n}$'s are on the same plane, the normal vector of the plane, ${}^{C}_{\pi}\mathbf{n}$, is orthogonal to these vectors, i.e. ${}^{C}_{\pi}\mathbf{n}^T \cdot \mathbf{i}_{m,n} = 0$ for $n = 1 \sim N$, $m = 1 \sim M$. The resulting equations are:

$$ \mathbf{Q}_\mathbf{n} \mathbf{x}_\mathbf{n} = \begin{bmatrix} \hat{\mathbf{i}}_{1,1}^T \\ \vdots \\ \hat{\mathbf{i}}_{M,N}^T \end{bmatrix} \cdot {}^{C}_{\pi}\mathbf{n} = 0 \quad (18) $$

For $N \times M$ vectors, the dimension of $\mathbf{Q}_\mathbf{n}$ is $(NM) \times 3$, and a unique solution $\mathbf{x}_\mathbf{n}$ exists if the $\hat{\mathbf{i}}_{m,n}$'s are not parallel. If the numbers of translating vectors in each orientation are identical, equation (18) has $N \times M$ equations. The solution

is the eigenvector corresponding to the smallest eigenvalue of the matrix $\mathbf{Q}_\mathbf{n}^T\mathbf{Q}_\mathbf{n}$ and is normalized to a unit vector.

(4) Find laser directions w.r.t. the camera

As shown in Figure 3, the vector $\mathbf{j}_{m,n}$ projects onto vector $\mathbf{i}_{m,n}$ along the laser beam direction $\mathbf{u}_m$. Figure 4 shows the relationships by placing the vectors together on the plane.

Therefore:

$$\mathbf{i}_{m,n} = \mathbf{j}_{m,n} + d_{m,n}\mathbf{u}_m \tag{19}$$

where:

$$d_{m,n} = -\frac{\mathbf{j}_{m,n}^T \cdot \mathbf{n}_\pi}{\mathbf{u}_m^T \cdot \mathbf{n}_\pi},$$

which is equivalent to:

$$\mathbf{i}_{m,n} = \mathbf{G}_m \cdot \mathbf{j}_{m,n} = \left(\mathbf{I} - \frac{\mathbf{u}_m\mathbf{n}_\pi^T}{\mathbf{u}_m^T\mathbf{n}_\pi}\right)\cdot \mathbf{j}_{m,n} \tag{20}$$

After attaching the coordinate systems:

$${}^C\mathbf{i}_{m,n} = {}^C\mathbf{G}_m \cdot {}^C\mathbf{j}_{m,n} = {}^C\mathbf{G}_m \cdot {}^C_B\mathbf{R} \cdot {}^B\mathbf{j}_{m,n}. \tag{21}$$

Let a transformation matrix be defined as:

$$\hat{\mathbf{G}}_m = \begin{bmatrix} \hat{\bar{\mathbf{g}}}_1 \\ \hat{\bar{\mathbf{g}}}_2 \\ \hat{\bar{\mathbf{g}}}_3 \end{bmatrix}_m = {}^C\mathbf{G}_m \cdot {}^C_B\mathbf{R} = \begin{bmatrix} {}^C\bar{\mathbf{g}}_1 \\ {}^C\bar{\mathbf{g}}_2 \\ {}^C\bar{\mathbf{g}}_3 \end{bmatrix}_m {}^C_B\mathbf{R} \tag{22}$$

Equation (21) can be rewritten as:

$$\begin{aligned}\mathbf{A}_{m,n}\mathbf{x}_{\mathbf{g},m} &= \begin{bmatrix} {}^B\mathbf{j}_{m,n}^T & 0 & \mathbf{0} \\ 0 & {}^B\mathbf{j}_{m,n}^T & \mathbf{0} \\ 0 & 0 & {}^B\mathbf{j}_{m,n}^T \end{bmatrix} \begin{bmatrix} \hat{\bar{\mathbf{g}}}_1^T \\ \hat{\bar{\mathbf{g}}}_2^T \\ \hat{\bar{\mathbf{g}}}_3^T \end{bmatrix}_m = \mathbf{b}_{m,n} \\ &= {}^C\mathbf{i}_{m,n}.\end{aligned} \tag{23}$$

The N translating vectors in mth orientation form:

$$\begin{bmatrix} \mathbf{A}_1 \\ \vdots \\ \mathbf{A}_N \end{bmatrix}_m \mathbf{x}_{\mathbf{g},m} = \begin{bmatrix} \mathbf{b}_1 \\ \vdots \\ \mathbf{b}_N \end{bmatrix}_m. \tag{24}$$

The ${}^B\mathbf{j}_{m,n}$'s are from the manipulator commands and ${}^C\hat{\mathbf{i}}_{m,n}$'s replacing ${}^C\mathbf{i}_{m,n}$'s in equation (24) are obtained from previous procedure (equation (17)). The solution is calculated by least squares method and is rearranged into a 3×3 matrix, which is proportional to $\hat{\mathbf{G}}_m$ with a scalar $1/\lambda_m$. This matrix is denoted as $\tilde{\mathbf{G}}_m = \hat{\mathbf{G}}_m/\lambda_m$. According to equation (24), at least three non-coplanar robot translations are required to obtain a unique solution.

Figure 4 Intersection of a laser beam and a plane

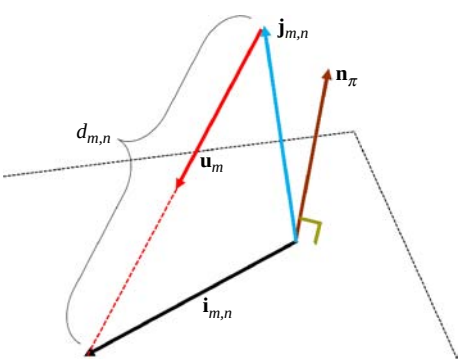

The rotation term can be eliminated algebraically by multiplying $\tilde{\mathbf{G}}_m$ with its transpose. Let $\tilde{\mathbf{u}}_m = \mathbf{u}_m/\lambda_m\mathbf{u}_m^T\mathbf{n}_\pi$. According to equations (20) and (21):

$$\tilde{\mathbf{G}}_m\tilde{\mathbf{G}}_m^T = \left(\left(\tilde{\mathbf{u}}_m^T\mathbf{n}_\pi\right)^2\mathbf{I} - \tilde{\mathbf{u}}_m^T\mathbf{n}_\pi \cdot \tilde{\mathbf{u}}_m\mathbf{n}_\pi^T - \tilde{\mathbf{u}}_m^T\mathbf{n}_\pi \cdot \mathbf{n}_\pi\tilde{\mathbf{u}}_m^T + \tilde{\mathbf{u}}_m\tilde{\mathbf{u}}_m^T \right) \tag{25}$$

Each element on the left side equal to relative element on the right side forms a quadratic equation of three arguments that are three elements of $\tilde{\mathbf{u}}_m$. Since the matrix $\tilde{\mathbf{G}}_m\tilde{\mathbf{G}}_m^T$ is symmetric, it contains six quadratic equations and their coefficients are composed of the elements of the normal vector $\mathbf{n}_\pi$. The solution of these equations is $\tilde{\mathbf{u}}_m$. Normalizing $\tilde{\mathbf{u}}_m$ to a unit vector gives the laser direction $\mathbf{u}_m$ at the mth orientation in the camera frame.

(5) Find the rotation matrix between the camera and robot

Since rotation between the robot base frame and the camera frame is unique, all vectors at different hand orientations are subject to this relation. From equation (22), $\hat{\bar{\mathbf{g}}}_{a,m}^T = {}^B_C\mathbf{R}\,{}^C\bar{\mathbf{g}}_{a,m}^T$ for $a = 1 \sim 3$ and $m = 1 \sim M$. Rotation ${}^B_C\mathbf{R}$ represented by a unit quaternion is applied to obtain a linear form of this equation (Horn, 1987). The quaternion is generally defined as $\dot{q} = q_0 + q_1 i + q_2 j + q_3 k$ and can also be written in a vector $\mathbf{q} = [q_0 \quad q_1 \quad q_2 \quad q_3]^T$. Let $\hat{\mathbf{v}} = [0 \quad \hat{\bar{\mathbf{g}}}]^T$ and $\mathbf{v} = [0 \quad {}^C\bar{\mathbf{g}}]^T$:

$$\hat{\mathbf{v}} = \mathbf{q}\otimes\mathbf{v}\otimes\mathbf{q}^{-1} \tag{26}$$

where $\otimes$ represents quaternion multiplication and $\mathbf{q}^{-1}$ is the inverse of the quaternion. Equation (26) is equal to:

$$\hat{\mathbf{v}}\otimes\mathbf{q} - \mathbf{q}\otimes\mathbf{v} = (E(\hat{\mathbf{v}}) - W(\mathbf{v}))\mathbf{q} = 0 \tag{27}$$

where:

$$E(\mathbf{v}) = \begin{bmatrix} v_0 & -v_1 & -v_2 & -v_3 \\ v_1 & v_0 & -v_3 & v_2 \\ v_2 & v_3 & v_0 & -v_1 \\ v_3 & -v_2 & v_1 & v_0 \end{bmatrix} \quad \text{and}$$

$$W(\mathbf{v}) = \begin{bmatrix} v_0 & -v_1 & -v_2 & -v_3 \\ v_1 & v_0 & v_3 & -v_2 \\ v_2 & -v_3 & v_0 & v_1 \\ v_3 & v_2 & -v_1 & v_0 \end{bmatrix}$$

The equation for all vectors rotating from camera frame to robot base frame is:

$$\mathbf{Q}_\mathbf{q}\mathbf{x}_\mathbf{q} = \begin{bmatrix} E(\hat{\mathbf{v}}_{1,1}) - W(\mathbf{v}_{1,1}) \\ \vdots \\ E(\hat{\mathbf{v}}_{3,M}) - W(\mathbf{v}_{3,M}) \end{bmatrix}_{(12M)\times 4} {}^B_C\mathbf{q} = 0 \tag{28}$$

The solution is the eigenvector corresponding to the smallest eigenvalue of the matrix $\mathbf{Q}_\mathbf{q}^T\mathbf{Q}_\mathbf{q}$ and is normalized to satisfy ${}^B_C\mathbf{q}^T{}^B_C\mathbf{q} = 1$. The rotation matrix from the camera coordinate system to the robot base coordinate system is then obtained from:

$$ {}^B_C\mathbf{R} = {}^B_C \begin{bmatrix} 1-2q_2^2-2q_3^2 & 2(q_1q_2+q_3q_0) & 2(q_1q_3-q_2q_0) \\ 2(q_1q_2-q_3q_0) & 1-2q_1^2-2q_3^2 & 2(q_2q_3+q_1q_0) \\ 2(q_1q_3+q_2q_0) & 2(q_2q_3-q_1q_0) & 1-2q_1^2-2q_2^2 \end{bmatrix}. \tag{29} $$

(6) Find the laser direction w.r.t the end-effector

The laser emitter is rigidly attached on the end-effector and the laser beam direction is ${}^E_\Lambda\mathbf{u}$ relative to the end-effector frame. The laser beam direction at the mth hand orientation in the camera frame is:

$$ {}^C\mathbf{u}_m = {}^C_B\mathbf{R}\,{}^B_E\mathbf{R}_m\,{}^E_\Lambda\mathbf{u}. \tag{30} $$

Hence, the M orientations lead to an equation:

$$ \mathbf{A}_\mathbf{u}\mathbf{x}_\mathbf{u} = \begin{bmatrix} {}^C_B\mathbf{R}\,{}^B_E\mathbf{R}_1 \\ \vdots \\ {}^C_B\mathbf{R}\,{}^B_E\mathbf{R}_M \end{bmatrix} {}^B_\Lambda\mathbf{u} = \mathbf{b}_\mathbf{u} = \begin{bmatrix} {}^C\mathbf{u}_1 \\ \vdots \\ {}^C\mathbf{u}_M \end{bmatrix}. \tag{31} $$

The solution can be calculated by least square method.

(7) Find the scale factors of the homogeneous matrix and the translations of the laser and the camera

The laser beam is emitted from its origin in hand to the position on the plane. At mth orientation and kth translation, the laser is at position ${}^B_\Lambda\mathbf{p}_{m,k} = {}^B_E\mathbf{R}_m\,{}^E_\Lambda\mathbf{T} + {}^B_E\mathbf{T}_{m,k}$ in the robot base frame, and the laser spot is at ${}^C_\pi\mathbf{p}_{m,k} = \lambda_m \cdot {}^C_\pi\hat{\mathbf{p}}_{m,k} = \lambda_m(w^C_{1,m,k}\hat{\mathbf{i}}_{m,1} + \cdots + w^C_{N,m,k}\hat{\mathbf{i}}_{m,N} + {}^C\hat{\mathbf{T}}_m)$ in the camera frame. After transforming the laser position from the robot base frame to the camera frame, the laser beam from the robot side to the plane is:

$$ {}^C\mathbf{t}_{m,k} = {}^C_B\mathbf{R}\,{}^B_\Lambda\mathbf{p}_{m,k} + {}^C_B\mathbf{T}_{m,k} - {}^C_\pi\mathbf{p}_{m,k} \tag{32} $$

which is parallel to ${}^C\mathbf{u}_m$, so ${}^C\mathbf{u}_m \times {}^C\mathbf{t}_{m,k} = 0$. Consequently:

$$ \begin{bmatrix} \lfloor {}^C\mathbf{u}_m \rfloor_\times {}^C_B\mathbf{R}\,{}^B_E\mathbf{R}_m & \lfloor {}^C\mathbf{u}_m \rfloor_\times & -\lfloor {}^C\mathbf{u}_m \rfloor_\times \hat{\mathbf{H}}_m \begin{bmatrix} \mathbf{w}_{m,k} \\ 1 \end{bmatrix} \end{bmatrix} \begin{bmatrix} {}^E_\Lambda\mathbf{T} \\ {}^C_B\mathbf{T} \\ \lambda_m \end{bmatrix} = -\lfloor {}^C\mathbf{u}_m \rfloor_\times {}^C_B\mathbf{R}\,{}^B_E\mathbf{T}_{m,k} \tag{33} $$

where:

$$ \lfloor {}^C\mathbf{u}_m \rfloor_\times = \begin{bmatrix} 0 & -{}^Cu_{3,m} & {}^Cu_{2,m} \\ {}^Cu_{3,m} & 0 & -{}^Cu_{1,m} \\ -{}^Cu_{2,m} & {}^Cu_{1,m} & 0 \end{bmatrix}. $$

Since ${}^E_\Lambda\mathbf{T} = {}^E_\Lambda[0 \quad y \quad z]^T$, the first column of the most left matrix should be eliminated. For all $M \times K$ points, the equation is $\mathbf{A}_\mathbf{T}\mathbf{x}_\mathbf{T} = \mathbf{b}_\mathbf{T}$ where $\mathbf{x}_\mathbf{T} = [{}^E_\Lambda x \;\; {}^E_\Lambda y \;\; {}^C_B\mathbf{T} \;\; \lambda_1 \;\; \cdots \;\; \lambda_M]^T$, $\mathbf{A}_\mathbf{T}$ is $(3MK) \times (5 + M)$, and $\mathbf{b}_\mathbf{T}$ is $(3KM) \times 1$. The solution is calculated by least square method.

(8) Find the plane w.r.t. the camera frame

Since the plane normal vector is already obtained in the third step, the position of the plane can be calculated. A better estimation can be obtained by averaging the results computed in the previous steps. The plane is:

$$ {}^C_\pi\mathbf{a} = \left(\sum_{m=1}^{M} \sum_{k=1}^{K} {}^C_\pi\mathbf{p}^T_{m,k} \cdot {}^C_\pi\mathbf{n} \right) {}^C_\pi\mathbf{n}. \tag{34} $$

in the camera frame.

Nonlinear optimization

The closed-form solution provides a good estimation for the system. However, errors may propagate during the solution procedure. A nonlinear optimization problem is therefore introduced to refine the results. The laser projecting points are constrained on the plane and observed by the camera under different arm poses; this yields the following optimization problem:

$$ \min_S \sum_{m=1}^{M} \sum_{k=1}^{K} \left\| \mathbf{m}_{m,k} - \hat{\mathbf{m}}\left(S, {}^B_E\mathbf{R}_{m,k}, {}^B_E\mathbf{T}_{m,k}\right) \right\|^2 \tag{35} $$

where ${}^B_E\mathbf{R}_{m,k}$ and ${}^B_E\mathbf{T}_{m,k}$ are obtained from the (m, k)th command of the manipulator; $\mathbf{m}_{m,k}$ is the estimated point position from the (m, k)th image; $\hat{\mathbf{m}}(\cdot)$ is the prediction of the projection position in the image according to equations (1)-(9) and; and S is the set of parameters to be refine, which include ${}^C_B\theta$, ${}^C_B\phi$, ${}^C_B\varphi$, ${}^C_B\mathbf{T}$, ${}^E_\Lambda\theta$, ${}^E_\Lambda\phi$, ${}^E_\Lambda y$, ${}^E_\Lambda z$, and ${}^C_\pi\mathbf{a}$. Equation (35) is a nonlinear minimization problem that can be solved using the Levenberg-Marquardt method.

Calibration procedure

The following calibration procedure is proposed:

1. Attach a laser pointer to the end-effector of the manipulator or to the tool.
2. Move the end-effector to one position. Rotate the end-effector to point the laser beam toward the plane, and let the laser spot move to one location in the camera field of view. Record the robot pose, and capture the camera image.
3. Translate but do not rotate the end-effector along several directions. Allow the end-effector stop at multiple positions in each direction while keeping the laser spot in the camera field of view. Record the robot pose, and capture the camera image at each pose.
4. Repeat steps 2 and 3 until sufficient data are collected.
5. Extract the laser spot in each image to find its image position.
6. Estimate the parameters using the closed-form solution.
7. Refine the solution using the nonlinear optimization.

Experimental results

Simulations

To validate the proposed method, simulations were performed under different noise levels and with different numbers of samples. The camera intrinsic parameters were set to $f_u = 543$, $f_v = 543$, $\alpha_c = 0.05$, $u_0 = 320$, and $v_0 = 240$. The actual parameters in all cases were ${}^B_C\theta = -90°$, ${}^B_C\phi = -10°$, ${}^B_C\varphi = -170°$, ${}^B_C\mathbf{T} = [510, 151, 430]^T$ (mm), ${}^E_\Lambda\theta = 21.80°$, ${}^E_\Lambda\phi = 53.39°$, and ${}^E_\Lambda\mathbf{T} = [0, -10, 30]^T$ (mm). The performances of the proposed method are assessed

Industrial Robot: An International Journal
Volume 39 · Number 2 · 2012 · 197–207

by comparing to Dornaika and Horaud's method (1998). Dornaika and Horaud's method is representative of simultaneous eye-to-hand and tool-on-hand calibration methods due to its effectiveness and accuracy. Since the system configurations for these two methods are different, the data are generated in different ways. As in Figure 5(a), the end-effector is confined to move in a part of robot workspace, the gray region, in which the laser beam can reasonably be aimed to the top surface of working plane. For the Dornaika and Horaud's method, the robot is confined to move a 3D reference object on hand in the gray region, a part of the camera field of view in Figure 5(b). The reference object was composed of ten points and the distance between two points on the same axis was 2.5 cm. The transformation between the object frame and the hand frame was with paramters, ${}^{E}_{O}\theta = -10°$, ${}^{E}_{O}\phi = -20°$, ${}^{E}_{O}\varphi = -45°$, ${}^{E}_{O}\mathbf{T} = [50, -20, 70]^{T}$(mm), and this transformation will be calibrated in their method.

Figure 5 Side view of simulation setups of (a) the proposed method and (b) the Dornaika and Horaud's method

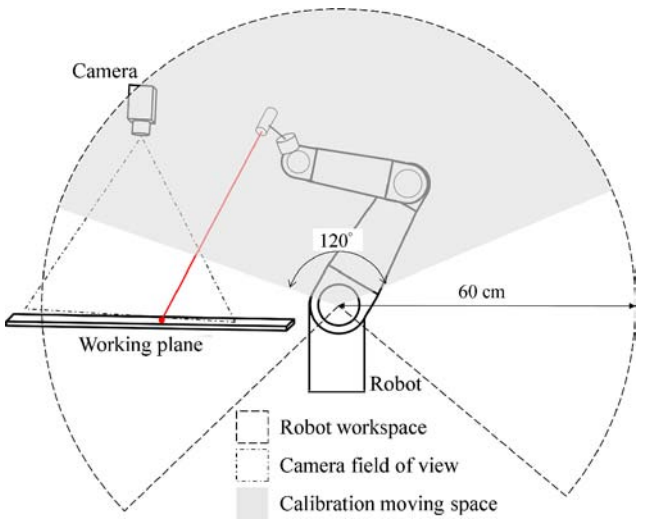

(a)

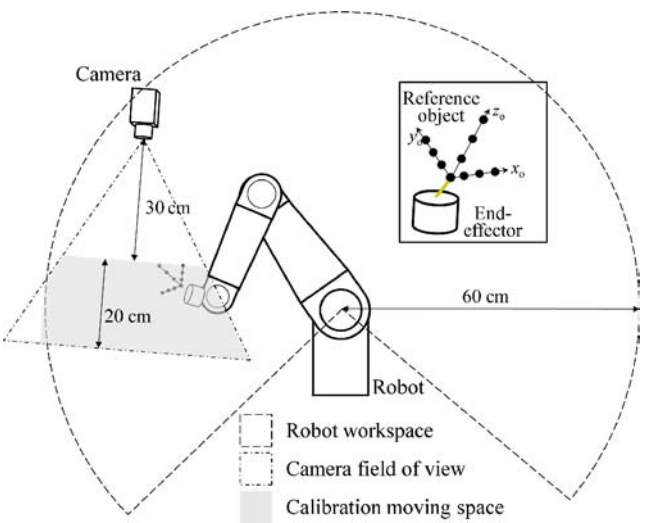

(b)

The effect of noise in image positions is tested. For the proposed method, the orientation of a plane positioned about 550 mm in front of the camera is determined as follows: the plane is initially parallel to the image plane and then it is rotated around the x-axis and then the y-axis, each at a random angle of the range of -5 to 5°. Following the recommended procedure described above, the end-effector is moved to a random position in the confined space and it is rotated to point the laser beam to form a laser spot on the plane at a random location. Then, the end-effector is translated to three random directions, along each of which are three translations. The steps 2 and 3 are performed five times. In total, 50 $(5 \times (1 + 3 \times 3))$ samples are generated with hand poses and camera measurements. For the Dornaika and Horaud's method, five random hand poses are generated by randomly tanslating and rotating the hand about random rotational axes, each at a random angle in -15 to 15°, to obtain 50 (5×10) point samples. The poses of the object in the camera frame are calculated by using a function compute_extrinsic in *Camera Calibration Toolbox for Matlab* (Bouguet, 2010). Each point measurement is contaminated by Gaussian noise with a zero mean and standard deviation. Errors in estimated parameters are presented as percentage of deviation from actual parameters. In this test, the noise level (i.e. standard deviation) varies from 0 to 1 pixel. For each noise level, 100 independent trials were performed. Figure 6(a) shows the closed-form solution results, and Figure 6(b) shows the results after refinement by using the nonlinear optimization methods. The rotation and translation errors are the Frobenius norms of the difference between the true and estimated ${}^{B}_{C}\mathbf{T}$ and ${}^{B}_{C}\mathbf{R}$, and the relative errors are calculated as $\|\mathbf{T}_{estimated} - \mathbf{T}_{true}\|_F / \|\mathbf{T}_{true}\|_F$ and $\|\mathbf{R}_{estimated} - \mathbf{R}_{true}\|_F / \|\mathbf{R}_{true}\|_F$ in percentages, respectively. The calculation results show that average errors increase as the noise levels increase, but average relative errors in the refined results are less than 1 percent when the noise level is less than 1 pixel. The Dornaika and Horaud's closed-form solution is less sensitive to noise in this condition; however, the performances of the two methods are similar after nonlinear optimization.

Performance is also compared using different numbers of samples. Three to 12 hand orientations, each with three translating directions and three hand positions along each direction, are generated for our proposed method. These movements generated 30-120 samples. The plane poses at each trail are randomly determined in the same way as described above. Likewise, three to 12 random hand poses are generated for the Dornaika and Horaud's method. Zero mean Gaussian noise with a 0.5-pixel standard deviation is added to each image position. For different numbers of samples, 100 independent trials are performed, and average errors are calculated (Figure 7). The relative translation errors are larger than the rotation errors in both methods, because of error propagation in the closed-form solution. The results indicate that errors decrease as number of samples increases. Nonlinear optimization with 120 samples provides a better result and has about 20 times less error than the closed-form solution does in our proposed approach. After optimization, the accuracy of the propose approach is better with smaller number of samples, and the accuracies of two approaches are approximate with large number of samples even though our proposed approach has one more unknown parameter, i.e. one degree of freedom, than Dornaika and Horaud's approach does.

Figure 6 Relative errors with respect to the noise level

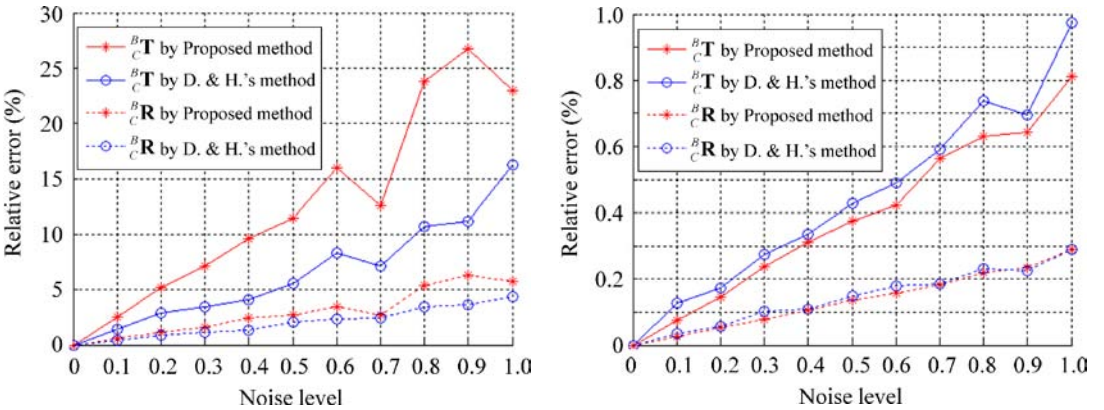

Notes: (a) Closed-form solution; (b) nonlinear optimization

Figure 7 Relative errors with respect to the number of samples

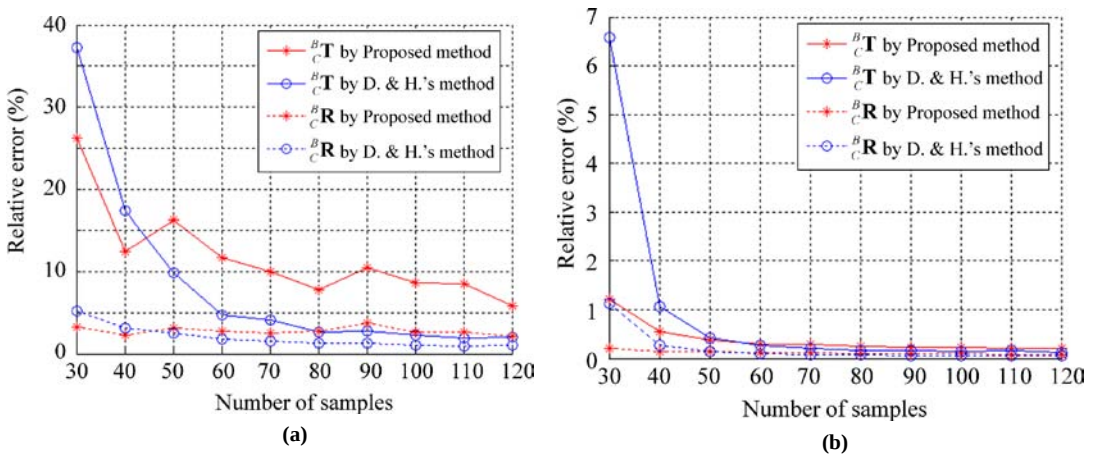

Notes: (a) Closed-form solution; (b) nonlinear optimization

Real data

The manipulator used in this study, a TX60 with a CS8 controller, was manufactured by Stäubli Inc. The camera was a Panasonic WV-CP 480 CCD camera with an adjustable lens, and its resolution is 640 × 480 pixels. As in Figure 8(a), the camera was about 100 cm away from the robot base and it looked down to a working plane. The working plane was roughly 110 cm away from the manipulator. The area of the plane within the camera view scope was about 20 × 15 cm. The laser pointer was a laser diode with an adjustable lens which is attached on the robot tool, as in Figure 8(b). Figure 8(c) shows the connection between devices. The camera signal in NTSC format was transmitted to the frame grabber, RTV-24, through a coaxial cable. The frame grabber card is inside the computer. A Visual C program in the computer can save images, send robot commends to the CS8 controller and receive robot status from the controller through an Ethernet. The tech pendant ran a program in the controller to move the robot manipulator accordingly and to send data back. This proposed calibration method with a function of the laser spot extraction was implemented in MATLAB in this computer.

Camera intrinsic parameters were estimated by applying *Camera Calibration Toolbox for Matlab* (Bouguet, 2010). This camera calibration was performed with a pattern of $35(5 \times 7)$ grids; each grid was $15 \times 15\,\text{mm}^2$. In total, 40 images of the pattern under different orientations are taken. The calibrated camera intrinsic parameter values were $f_u = 2{,}283.161$, $f_v = 2{,}283.039$, $\alpha_c = 0$, $u_0 = 269.910$, $v_0 = 248.321$, $\kappa_1 = 0.044$, $\kappa_2 = 3.869$, $\rho_1 = -0.002$, $\rho_2 = -0.009$.

We complied with the recommended procedure to manipulate the end-effector. The end-effector was moved to one position and then moved along three different directions under each hand orientation. Three positions along each direction were generated to obtain ten image positions per orientation. Nine different hand orientations were performed. Each hand pose and its relative image were recorded. In total, 90 samples are collected. All movements were intended to project the laser beam onto the planar object and in camera field of view. Table I shows the results. Four tests were conducted.

Figure 8 Experimental setup

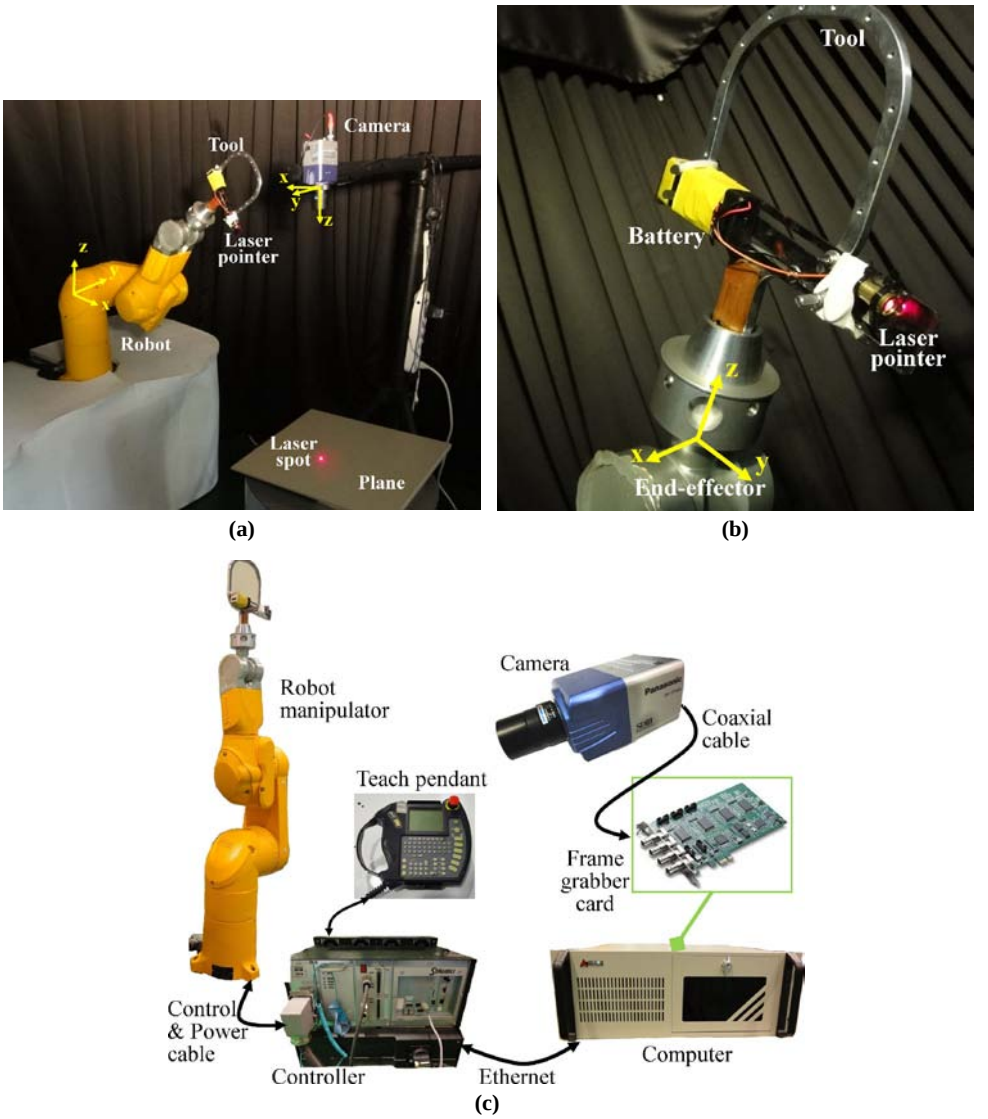

Notes: (a) Side view; (b) a laser pointer attached on the end-effector; (c) connection of the devices

The first column in the first test, labeled Initial, is the estimation of the closed-form solution. The columns, labeled Refined, are the estimation of nonlinear optimization, and the columns, labeled σ, are the standard deviation, indicating the uncertainty of the refined result. The second and third tests used more samples, including the 30 initialization samples, to refine the values from the first test. In the fourth test, 50 samples were selected by outlier rejection based on the differences between estimated and predicted image positions using the refined parameters from the test of total 90 samples, i.e. 50 samples with the smallest pixel error were selected. The outlier rejection can exclude some samples that are seriously corrupted by the effect of laser speckle. In each test, the last row showed the root mean square (RMS) of the distance from the estimated image positions to the predicted image positions. The results are consistent with simulation results; moreover, the RMS value is significantly lower in the result with outlier rejection. Figure 9 shows the extrinsic results for the last test. The last column shows the plane with respect to camera frame by a pattern grid superimposed on the plane in the camera calibration stage. This can be used as criteria for validating the test results shown in other columns, are consistent.

Conclusion

This work develops a new calibration method for accurately estimating the configuration between a camera and a robot. This technique is accomplished through a laser pointer. Since the laser is rigidly installed and the plane is fixed, camera measurements of light spots, which the laser beam projected onto the plane, must obey the geometrical constraints. Based on the constraints, the proposed closed-form solution obtains initial values, and the nonlinear optimization can be applied to refine these values. Computer simulations are used to validate the calibration method and to analyze the performance in different conditions. Experimental results using real data verify that the proposed method is effective when the hand

Table I Results with real data of different number of samples

	30 samples			40 samples		
Parameter	*Initialized*	*Refined*	σ	*Refined*	Σ	*Unit*
$({}^{B}_{C}\theta, {}^{B}_{C}\phi, {}^{B}_{C}\varphi)$	(−100.14, −3.29, −172.69)	(−102.55, −6.15, −174.22)	(0.09, 0.57, 0.59)	(−102.56, −5.95, −173.72)	(0.07, 0.42, 0.48)	Degree
${}^{B}_{C}T^{T}$	(1,343.73, −4.34, 319.28)	(965.56, −47.41, 440.90)	(5.14, 8.01, 11.10)	(973.66, −40.87, 437.85)	(2.99, 3.44, 8.85)	mm
$({}^{E}_{\Lambda}\theta, {}^{E}_{\Lambda}\phi)$	(−89.93, 80.21)	(−91.15, 84.45)	(0.03, 0.07)	(−91.15, 84.40)	(0.01, 0.02)	Degree
${}^{E}_{\Lambda}T^{T}$	(−30.14, 0.00, 423.31)	(8.55, 0, 135.06)	(0.87, 0.00, 5.07)	(7.61, 0.00, 138.99)	(0.29, 0, 0.89)	mm
${}^{C}_{\pi}a^{T}$	(−70.39, 55.95, 690.76)	(−50.57, 35.52, 705.07)	(0.81, 0.68, 3.48)	(−58.43, 34.04, 703.45)	(0.59, 0.47, 1.49)	mm
RMS	30.32	1.0626		1.0923		Pixel
	50 samples		50 samples with outlier rejection			
Parameter	*Refined*	σ	*Refined*	σ	*Camera calibration stage*	*Unit*
$({}^{B}_{C}\theta, {}^{B}_{C}\phi, {}^{B}_{C}\varphi)$	(−102.60, −5.88, −173.53)	(0.07, 0.39, 0.45)	(−102.55, −6.00, −173.90)	(0.06, 0.35, 0.38)	N/A	Degree
${}^{B}_{C}T^{T}$	(976.59, −38.35, 436.62)	(2.83, 3.16, 8.17)	(973.96, −44.85, 439.26)	(2.44, 2.59, 6.85)	N/A	mm
$({}^{E}_{\Lambda}\theta, {}^{E}_{\Lambda}\phi)$	(−91.13, 84.36)	(0.01, 0.02)	(−91.13, 84.34)	(0.01, 0.01)	N/A	Degree
${}^{E}_{\Lambda}T^{T}$	(7.49, 0.00, 140.77)	(0.30, 0.00, 0.77)	(9.74, 0.00, 140.79)	(0.23, 0.00, 0.30)	N/A	mm
${}^{C}_{\pi}a^{T}$	(−61.34, 33.18, 702.78)	(0.59, 0.47, 1.47)	(−58.03, 36.93, 704.33)	(0.38, 0.26, 0.95)	(−58.54, 39.03, 703.95)	mm
RMS	1.1494		0.9568			Pixel

Note: N/A – not available

Figure 9 Extrinsic results

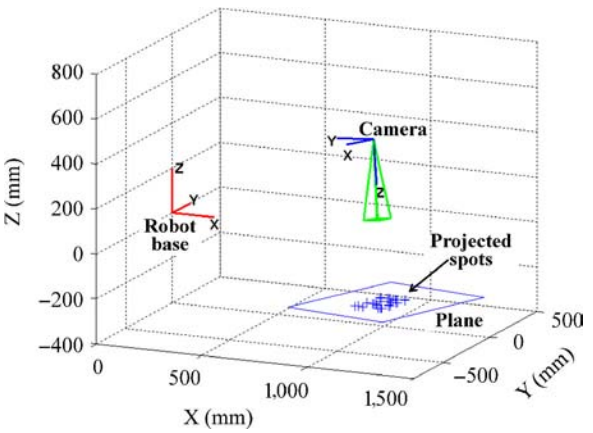

cannot be viewed by the camera, and the good agreement between the results using simulation data and real data validates the proposed method.

References

Abdel-Aziz, Y.I. and Karara, H.M. (1971), "Direct linear transformation into object space coordinates in close-range photogrammetry", *Proceedings of the Symposium on Close-range Photogrammetry, Urbana, IL, USA*, pp. 1-18.

Andreff, N., Horaud, R. and Espiau, B. (2001), "Robot hand-eye calibration using structure-from-motion", *The International Journal of Robotics Research*, Vol. 20, pp. 228-48.

Bacakoglu, H. and Kamel, M.S. (1997), "A three-step camera calibration method", *IEEE Transactions on Instrumentation and Measurement*, Vol. 46 No. 5, pp. 1165-72.

Bouguet, J.-Y. (2010), *Camera Calibration Toolbox for Matlab*, available at: www.vision.caltech.edu/bouguetj/calib_doc/ (accessed 15 December 2010).

Brown, D. (1971), "Close-range camera calibration", *Photogrammetric Engineering*, Vol. 37, pp. 855-66.

Chou, J.C.K. and Kamel, M. (1988), "Quaternions approach to solve the kinematic equation of rotation, AaAx=AxAb, of a sensor-mounted robotic manipulator", *IEEE International Conference on Robotics and Automation, Philadelphia, PA*, pp. 656-62.

Dornaika, F. and Horaud, R. (1998), "Simultaneous robot-world and hand-eye calibration", *IEEE Transactions on Robotics and Automation*, Vol. 14, pp. 617-22.

Gatla, C.S., Lumia, R., Wood, J. and Starr, G. (2007), "Calibrating pan-tilt cameras in robot hand-eye systems using a single point", *IEEE International Conference on Robotics and Automation, Roma*, pp. 3186-91.

Ghosh, B.K., Tarn, T.J., Xi, N., Yu, Z. and Xiao, D. (1998), "Robotic motion planning and manipulation in an uncalibrated environment", *IEEE Robotics & Automation Magazine*, Vol. 5 No. 4, pp. 50-7.

Hartley, R.I. and Zisserman, A. (2003), *Multiple View Geometry in Computer Vision*, 2nd ed., Cambridge University Press, Cambridge.

Horaud, R. and Dornaika, F. (1995), "Hand-eye calibration", *The International Journal of Robotics Research*, Vol. 14, pp. 195-210.

Horn, B. (1987), "Closed-form solution of absolute orientation using unit quaternions", *Journal of the Optical Society of America A*, Vol. 4, pp. 629-42.

Hu, J.-S. and Chang, Y.-J. (2011), "Calibration of an eye-to-hand system using a laser pointer on hand and planar constraints", paper presented at IEEE International Conference on Robotics and Automation, Shanghai.

Hu, J.-S., Chien, M.-C., Chang, Y.-J., Chang, Y.-C., Su, S.-H., Yang, J.-J. and Kai, C.-Y. (2010), "A robotic ball catcher with embedded visual servo processor", paper presented at IEEE/RSJ International Conference on Intelligent Robots and Systems, Taipei, video paper.

Jordt, A., Siebel, N.T. and Sommer, G. (2009), "Automatic high-precision self-calibration of camera-robot systems", *IEEE International Conference on Robotics and Automation, Kobe*, pp. 1244-9.

Motai, Y. and Kosaka, A. (2008), "Hand-eye calibration applied to viewpoint selection for robotic vision", *IEEE Transactions on Industrial Electronics*, Vol. 55 No. 10, pp. 3731-41.

Motta, J.M.S.T., de Carvolho, G.C. and McMaster, R.S. (2001), "Robot calibration using a 3D vision-based measurement system with a single camera", *Robotics & Computer-Integrated Manufacturing*, Vol. 17 No. 6, pp. 487-97.

Shapiro, R. (1978), "Direct linear transformation method for three-dimensional cinematography", *Research Quarterly*, Vol. 49, pp. 197-205.

Shiu, Y.C. and Ahmad, S. (1987), "Finding the mounting position of a sensor by solving a homogeneous transform equation of the form AX=XB", *IEEE International Conference on Robotics and Automation*, pp. 1666-71.

Shiu, Y.C. and Ahmad, S. (1989), "Calibration of wrist-mounted robotic sensors by solving homogeneous transform equations of the form AX=XB", *IEEE Transactions on Robotics and Automation*, Vol. 5, pp. 16-29.

Sun, L., Liu, J., Sun, W., Wu, S. and Huang, X. (2004), "Geometry-based robot calibration method", *IEEE International Conference on Robotics and Automation, New Orleans, LA*, pp. 1907-12.

Tsai, R.Y. (1987), "A versatile camera calibration technique for high-accuracy 3D machine vision metrology using off-the-shelf TV cameras and lenses", *IEEE Journal of Robotics and Automation*, Vol. 3 No. 4, pp. 323-44.

Tsai, R.Y. and Lenz, R.K. (1988), "Real time versatile robotics hand/eye calibration using 3D machine vision", *IEEE International Conference on Robotics and Automation, Philadelphia, PA*, pp. 554-61.

Tsai, R.Y. and Lenz, R.K. (1989), "A new technique for fully autonomous and efficient 3D robotics hand/eye calibration", *IEEE Transactions on Robotics and Automation*, Vol. 5, pp. 345-58.

Wang, C.C. (1992), "Extrinsic calibration of a vision sensor mounted on a robot", *IEEE Transactions on Robotics and Automation*, Vol. 8, pp. 161-75.

Xu, H., Wang, Y., Chen, W. and Lu, J. (2008), "A self-calibration approach to hand-eye relation using a single point", *International Conference on Information and Automation, Zhangjiajie*, pp. 413-18.

Zhang, Z. (2000), "A flexible new technique for camera calibration", *IEEE Transaction on Pattern Analysis and Machine Intelligence*, Vol. 22 No. 11, pp. 1330-4.

Zhuang, H. and Roth, Z.S. (1991), "Comments on 'calibration of wrist-mounted robotic sensors by solving homogeneous transform equations of the form AX=XB'", *IEEE Transactions on Robotics and Automation*, Vol. 7, pp. 877-8.

Zhuang, H. and Shiu, Y.C. (1993), "A noise-tolerant algorithm for robotic hand-eye calibration with or without sensor orientation measurement", *IEEE Transactions on Systems, Man and Cybernetics*, Vol. 23, pp. 1168-75.

Zhuang, H., Roth, Z.S. and Sudhakar, R. (1994), "Simultaneous robot/world and tool/flange calibration by solving homogeneous transformation equations of the form AX=YB", *IEEE Transactions on Robotics and Automation*, Vol. 10, pp. 549-54.

Zhuang, H., Roth, Z.S., Xu, X. and Wang, K. (1993), "Camera calibration issues in robot calibration with eye-on-hand configuration", *Robotics & Computer-Integrated Manufacturing*, Vol. 10 No. 6, pp. 401-12.

Further reading

Wei, G.Q., Arbter, K. and Hirzinger, G. (1998), "Active self-calibration of robotic eyes and hand-eye relationships with model identification", *IEEE Transactions on Robotics and Automation*, Vol. 14, pp. 158-66.

About the authors

Jwu-Sheng Hu received the BS degree from the Department of Mechanical Engineering, National Taiwan University, Taiwan, in 1984, and the MS and PhD degrees from the Department of Mechanical Engineering, University of California at Berkeley, in 1988 and 1990, respectively. From 1991-1993, he was an Assistant Professor in the Department of Mechanical Engineering, Wayne State University, Detroit, USA where he received the Research Initiation Award from National Science Foundation. In 1993 he joined the Department of Electrical Engineering, National Chiao Tung University, Taiwan and became a Full Professor in 1998. He works in-part at the Industrial Technology Research Institute (ITRI) of Taiwan, where he serves as the advisor for the Intelligent Robotics program and is the principal investigator of large-scale robotics research projects funded by the Ministry of Economic Affairs. He also serves as an Advisor at the National Chip Implementation Center (CIC) of Taiwan for embedded system design applications. His current research interests include robotics, mechatronics, and embedded systems.

Yung-Jung Chang received the BS degree from the Department of Electrical Engineering, Yuan-Ze University, Taiwan, ROC and the MS degree from the Department of Control Engineering, National Chiao-Tung University (NCTU), Taiwan, ROC in 2005 and 2006, respectively. He is currently working toward the PhD degree at NCTU and works in-part at the Industrial Technology Research Institute (ITRI) of Taiwan. His research interests are mobile robot localization, modeling and calibration, computer vision, sensor fusion, and manipulator coordination. Yung-Jung Chang is the corresponding author and can be contacted at: nuo.ece95g@nctu.edu.tw